1-1-2008

# Prediction of passive intermodulation from coaxial connectors in microwave networks

Justin Henrie
*Purdue University*, jhenrie@purdue.edu

Andrew Christianson
*Purdue University*, christaj@purdue.edu

William J. Chappell
*School of Electrical and Computer Engineering, Birck Nanotechnology Center, Purdue University*, chappell@purdue.edu

# Prediction of Passive Intermodulation From Coaxial Connectors in Microwave Networks

Justin Henrie, *Student Member, IEEE*, Andrew Christianson, *Student Member, IEEE*, and William J. Chappell, *Member, IEEE*

***Abstract*—Coaxial connectors are frequently the dominant contributors to passive intermodulation (PIM) distortion in high-frequency networks. This paper reports on a circuit model enabling estimation of PIM distortion by coaxial connectors in the design of high-frequency networks. A method of modeling the effect of multiple point sources of PIM is applied to coaxial connectors, allowing the prediction of the PIM of networks with several connectors. Typical ranges of PIM produced by common connectors in a two-tone test are reported. The stability and repeatability of PIM produced by a single connector is examined. Nonlinear current–voltage curves for coaxial connectors are given that predict the PIM distortion output by coaxial connectors over a broad range of input powers. An experimental verification is given showing that PIM of a system can be predicted if the characteristics of the individual components are known.**

***Index Terms*—Coaxial connectors, communication system nonlinearities, passive intermodulation (PIM) distortion.**

## I. Introduction

PASSIVE intermodulation (PIM) is the distortion generated by the small nonlinear characteristics of passive RF components such as antennas and connectors. Passive nonlinearity is almost always a small effect, typically resulting in mixing products more than 100 dB down from the generating signal, which is typically insignificant compared to the levels of nonlinear distortion generated by active circuit components such as amplifiers. However, this large nonlinearity from active components can usually be eliminated by filtering. PIM distortion cannot always be eliminated by filtering and, thus, is often the dominant source of nonlinear distortion in high-powered systems. As a result of the great difference in power between transmitted and receive signals, PIM distortion levels as low as $-115$ dBm are potentially problematic sources of interference in many systems as the nonlinearity of passive components causes power at transmit frequencies to mix into the system's receive band [1]. PIM is most problematic in transmit/receive systems where transmit and receive bands are closely spaced. Frequency bands are becoming more densely populated, making PIM a growing concern in the wireless community.

The ability to predict total PIM of a system incorporating multiple PIM sources could have many applications, potentially enabling near-noise-floor PIM measurements and allowing for engineers to account for PIM in the design phase of the creation of a circuit. This paper describes an effort toward that end that focuses on the PIM produced by coaxial connectors.

Coaxial connectors are frequently the dominant contributors to PIM distortion in high-frequency networks [2]. While the linear properties of coaxial connectors are well understood [3], less is known about their nonlinear properties that contribute to PIM. A comprehensive methodology has also not been presented to model the collective contribution of coaxial connectors to the total PIM distortion of a system. In this paper, the third-order intermodulation (IM) product of coaxial connectors is investigated and modeled to show that when the level of PIM of individual connectors is known, the collective IM distortion due to coaxial connectors of the entire system can be predicted using simple circuit and transmission line theory. The general methodology is explained and used first to verify the accuracy of our measurement system. Specific third-order PIM levels are reported for some common connector types. Next, current–voltage relations for the nonlinearity of coaxial connectors are presented, which are used to predict the power level in the third IM product as a function of power passed through the connector. Lastly, an experiment using all the techniques outlined here is used to predict the total IM distortion of an RF network involving several different types of coaxial connectors as a function of power.

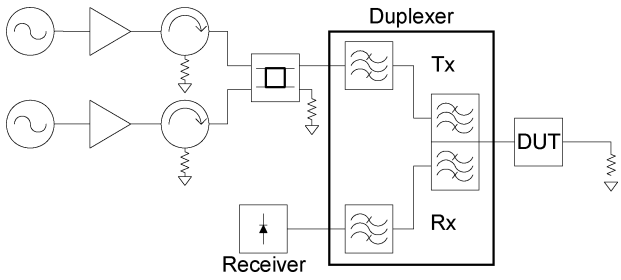


Fig. 1. Measurement system architecture.

## II. Analysis of Complex PIM-Producing Assemblies

All measurements in this study were taken using a Summitek SI-400C PIM distortion analyzer [4]. A simplified diagram of this measurement system is shown in Fig. 1. In this system, two high-powered carrier tones at frequencies $f_1$ and $f_2$ are

Manuscript received July 27, 2007; revised October 15, 2007. This work was supported in part by the U.S. Army Research Office as a Multi-disciplinary University Research Initiative on Standoff Inverse Analysis and Manipulation of Electronic Systems under Grant W911NF-05-1-0337.

J. Henrie and A. Christianson are with the Electrical and Computer Engineering Department, Purdue University, West Lafayette, IN 47907 USA (e-mail: justinhenrie@gmail.com; christaj@purdue.edu).

W. J. Chappell is with the Electrical and Computer Engineering Department and the Birck Nanotechnology Center, Purdue University, West Lafayette, IN 47907 USA (e-mail: chappell@purdue.edu).

Color versions of one or more of the figures in this paper are available online at http://ieeexplore.ieee.org.

Digital Object Identifier 10.1109/TMTT.2007.912166

transmitted through a duplexing filter to the device-under-test (DUT), which is terminated in a 50-$\Omega$ load. The purpose of the duplexer is to reject the high power carrier tones at the receiver port so that the low-level third-order IM product's signal can be detected. Spurious signals produced by PIM are generated in the DUT and propagate in both directions—"forward" to the matched termination and "reverse" to the duplexing filter (the sense of forward and reverse are taken relative to the propagation direction of the two large input tones generated by the external test system). The frequencies of the transmitted excitation tones and the measured IM products are set by the transmit (Tx) and receive (Rx) bands of the duplexing filter. The power of the reverse-propagating IM wave is measured at the receiver. For all measurements reported herein, the carrier tones were set at frequencies of 463 and 468 MHz, and unless otherwise specified were set at a transmit power of 42 dBm. The measured IM product was at the frequency $2f_1 - f_2 = 458$ MHz.

### A. Point-Source Model of PIM in Coaxial Assemblies

One of the difficulties in ascertaining the IM distortion (hereafter "IM" or "nonlinear distortion") level of any DUT is that the IM produced by the DUT is always accompanied by an unknown amount of "extraneous" IM power from the measurement system that interferes coherently with the IM generated by the DUT, potentially causing large measurement error. This extraneous IM power comes from two distinct mechanisms. First, unwanted IM is produced by nonlinearities in the measurement system. As much as possible, nonlinear components such as amplifiers and circulators are separated from the DUT by the duplexing filter shown in Fig. 1, which removes the nonlinear distortion of these components from the signal reaching the DUT and receiver. However, other system components such as cables, connectors, the dummy load, and the filter itself may generate IM, which can interfere with the IM produced by the DUT. This unwanted IM that is produced by the measurement system is called system residual IM and is discussed by Deats and Hartman in [5]. This system-generated IM sets the sensitivity floor of the instrument. The second mechanism that contributes to measurement error comes from the fact that most low-PIM loads are unterminated cables [6], which can have poor matching characteristics at lower frequencies as the quality of the match presented by such a load degrades with decreasing frequency. Reflections are caused by this impedance mismatch at the dummy load, which results in self-interference of the IM signal as investigated by Hienonen and Raisanen in [7]. The interference of both of these factors with the IM produced by a DUT is depicted in Fig. 2.

The IM resulting from the combination of all nonlinearities internal to the DUT results in two voltage waves: $V_{\rm DUT}^-$ is the reverse-propagating IM voltage wave, which is emitted at the reverse-facing port of the DUT, and $V_{\rm DUT}^+$ is the forward-propagating IM voltage wave produced at the forward-facing port of the DUT. The electrical lengths $l_{\rm back}$, $l_{\rm DUT}$, and $l_{\rm front}$ are all internal to the DUT. The length $l_{\rm front}$ is the distance from the reverse-facing port of the DUT to the first nonlinearity inside the DUT, $l_{\rm DUT}$ is the distance between the first and last nonlinearity inside the DUT, and $l_{\rm back}$ is the distance from the last nonlinearity and the forward-facing port of the DUT. The other

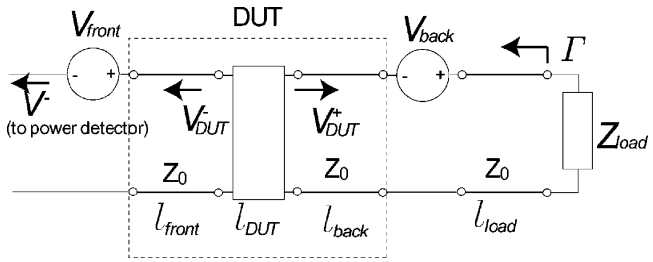


Fig. 2. Diagram of interaction between IM of a DUT, residual system IM, and finite reflection due to load mismatch at a single frequency.

voltage sources $V_{\rm front}$ and $V_{\rm back}$ represent the residual IM of the measurement system as it appears at the ports of the DUT. The electrical distance to the load $l_{\rm load}$ and load impedance $Z_{\rm load}$ are also included. The reverse-traveling voltage wave $V^-$ is measured by the system's power sensor.

Studies have found the PIM from coaxial connectors to be generated by *point-source*, as opposed to *distributed*, nonlinearities [2], [5], [8], i.e., the nonlinear distortion in a connector occurs at a specific point along the length of the connector (most likely at the metal–metal junction between the adapters). Following the discussion given in [5], it can be shown that in the forward direction, the voltage of all IM sources add in-phase so that the total IM voltage of a system with no reflections propagating in the forward direction is given as

$$V_{\rm IM}^+ = \sum_{n=1}^{N} V_n \tag{1}$$

where $V_n$ is the IM voltage generated by each point-source nonlinearity. When taking a reverse measurement, the phase difference of $\exp(j2\beta l_n)$ between IM sources must be included, where $l_n$ is the physical length between the first and $n$th IM source, and $\beta$ is the propagation constant. We thus find an expression for the total reverse-traveling IM voltage wave

$$V_{\rm IM}^- = \sum_{n=1}^{N} V_n \exp\left(j2\beta l_n\right). \tag{2}$$

With this in mind, the total reverse-traveling IM voltage wave at the receiver $V^-$, as shown in Fig. 2, is expressed as

$$\begin{aligned} V^- = {} & V_{\rm front} + V_{\rm DUT}^- \exp\left[j2\beta(l_{\rm front})\right] \\ & + V_{\rm back} \exp\left[j2\beta(l_{\rm back} + l_{\rm front} + l_{\rm DUT})\right] \\ & + \Gamma\left(V_{\rm front} + V_{\rm DUT}^+ + V_{\rm back}\right) \\ & \times \exp\left[j2\beta(l_{\rm front} + l_{\rm back} + l_{\rm load} + l_{\rm DUT})\right]. \end{aligned} \tag{3}$$

Again, $\beta$ is the propagation constant and all other symbols are taken from Fig. 2. The first three terms in (3) are reverse-traveling waves generated by the IM voltage sources $V_{\rm front}$, $V_{\rm back}$, and the reverse-traveling wave $V_{\rm DUT}^-$. The last term is the reflection of the forward traveling waves generated by $V_{\rm front}$, $V_{\rm back}$, and $V_{\rm DUT}^+$. In general, all parameters in (3) are unknown, except the load reflection coefficient $\Gamma$, which can be measured with a network analyzer.

We can use experimental data to solve for all unknowns in (3). Toward this end, we start by making the assumption that

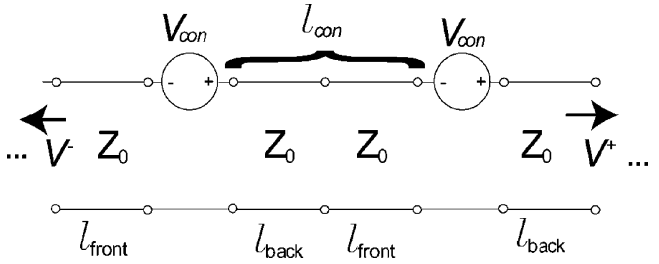


Fig. 3. Diagram of PIM at the third-order IM generated by a series of coaxial connectors (two depicted).

different connectors of the same make and model have the same PIM characteristics. Due to this, the $V^-_{\rm DUT}$, $V^+_{\rm DUT}l_{\rm front}$, $l_{\rm back}$, and $l_{\rm DUT}$ of different Pasternack Enterprises PE 9506 subminiature A (SMA) connectors used in the following experiment are assumed to have the same values.

As a point-source nonlinearity, we model the PIM of a coaxial connection as a voltage source between two sections of transmission line, the sum of whose lengths is equal to the total length of the connector. The voltage and phase of this source is dependent on the voltage and phase of the carrier tones incident upon it; the nature of this phase dependency is described in [5]. If we connect multiple PE 9506 connectors together in cascade, we are able model the interference between the connectors, as shown in Fig. 3.

Here, each voltage $V_{\rm con}$ source corresponds to the point nonlinearity of a single connection, and

$$l_{\rm con} = l_{\rm front} + l_{\rm back} \tag{4}$$

where $l_{\rm con}$ is the total electrical length of the connector and is easily measurable with a network analyzer. Since all connectors are assumed to have identical parameters, simple expressions for the voltage waves result from this cascade of connectors. For a stack of $N$ cascaded connectors, the reverse-traveling IM voltage wave $V^-$ will be

$$V^-_{\rm cascade} = \sum_{n=1}^{N} V_{\rm con} \exp\left[j2(n-1)\beta l_{\rm con}\right] \tag{5}$$

where $V_{\rm con}$ is the IM voltage produced in the connector and $l_{\rm con}$ is defined in (4). Since the forward-propagating waves generated by the connectors add in phase, the forward-traveling wave takes on the simple form

$$V^+_{\rm cascade} = NV_{\rm con} \tag{6}$$

and the internal electrical length of the DUT is

$$l_{\rm DUT} = (N-1)l_{\rm con}. \tag{7}$$

Equations (5) and (6) can now be used to give $V^-_{\rm DUT}$ and $V^+_{\rm DUT}$ in (3). Similarly, (4) and (7) can be used with (3) to yield

$$\begin{aligned} V^- = {} & V_{\rm front} + \sum_{n=1}^{N} V_{\rm con} \exp\left[j2\beta\left((n-1)l_{\rm con} + l_{\rm front}\right)\right] \\ & + V_{\rm back} \exp\left[j2\beta N l_{\rm con}\right] + \Gamma\left(V_{\rm front} + NV_{\rm con} + V_{\rm back}\right) \\ & \times \exp\left[j2\beta(Nl_{\rm con} + l_{\rm load})\right]. \end{aligned} \tag{8}$$

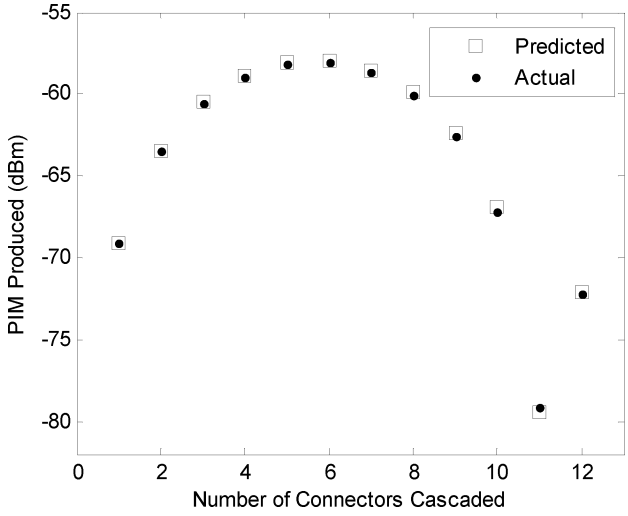


Fig. 4. Predicted versus measured IM (PIM) levels for cascades of coaxial connectors ranging from 1 to 12 connectors in length.

By varying the number of connectors $N$ in the cascade, we can generate an arbitrary number of independent equations based on (8). We can also measure the value of $V^-$ for each of these independent equations by simply constructing the appropriate cascade of connectors and measuring the IM that is generated in a two-tone test. Thus, we can solve for all unknown parameters in (3)–(8), determining both the characteristics of our DUT, as well as the residual IM sources in our measurement system.

### *B. Use of Model to Determine Measurement Accuracy*

Finding the exact value of all variables in (8) requires solving six independent nonlinear equations simultaneously. If instead one merely wishes to see whether or not the residual system IM and load reflection is influencing a measurement, the much simpler (5) can be used to predict what the relative magnitudes of the IM received from an assembly of known IM sources in the absence of any interference from the external system parameters such as system residual IM or load reflections.

A series of such cascades of coaxial connectors as described by (5) was tested on our measurement system for $N$ from 1 to 12, and compared against measurement. Fig. 4 shows the number of connectors in each cascade on the $x$-axis, and the power of the IM generated by these assemblies on the $y$-axis. The excellent agreement (maximum error: 0.4 dB) between the measured values and those predicted by (5) validates the assumptions made in constructing the model. Our first assumption was that the PIM of coaxial connectors is generated by a point nonlinearity at the connection between two coaxial connectors so that the entire connection could be modeled as a single voltage source between two lengths of transmission line, as shown in Fig. 3. Our second assumption was that the nonlinear characteristics of a group of SMA connections of the same manufacturer's model would be nearly equal to one another so that they would all produce identical IM under identical conditions.

Another observation that can be made for this particular test from Fig. 4 is that all sources of interference in this case are

negligible. Both the system residual IM and the reflections due to impedance mismatches in the system are very small in magnitude compared to the PIM produced by SMA connectors in this experiment. If this were not the case, the measured values shown would deviate from those predicted by (5). An analysis of (8) using the data in Fig. 4 showed that the residual IM of the system was at least 17 dB less than the IM of the SMA connections, corresponding to a maximum measurement error of 0.5 dB. Therefore, we have a high level of confidence in the accuracy of the data reported in Section III on the measured IM of SMA connections. A similar procedure was followed to determine the measurement error when measuring the IM produced by other types of connectors, and this measurement error is reported in the Section III.

## III. Measurements on Individual Coaxial Connectors

In order to predict the total IM behavior of a system comprising many coaxial connection IM sources, the individual contribution of each connection must be known. Once we have established that the residual IM floor is sufficiently small through a procedure such as outlined above, this can be determined through direct measurement. This section reports on such a measurement of some common types of coaxial connectors. The results of an experimental study of the IM characteristic of several common SMA and $N$ connectors are shown in Section III-A. Also, it is necessary that the characteristic of a connection when it is measured singly be treated as unchanged when it is incorporated into a large network. That is, the IM produced by a connection must be nearly constant over several mate/de-mate cycles. Section III-B reports on an experiment that establishes the validity of this assumption.

### A. Ranges of IM Produced by Individual Coaxial Connectors

We experimentally quantified the IM output of four common connector types in a two-tone test. Although this data is strictly useful only for a system design close to this power and frequency, the data is still of interest generally because the relative IM output of several different connector types can be seen. The coaxial connectors investigated were as follows.

- Pasternack Enterprises SMA connectors with gold plated inner conductor contact and outer conductor contact of nickel (part numbers PE 9103, PE 9081, and PE 9082) or stainless steel (PE 9433 and PE 9506). The level of system residual IM when testing these connectors gave a maximum measurement error of 0.5 dB.
- Pasternack Enterprises bayonet Neill-Concelman (BNC) connectors with gold-plated inner conductor contact and nickel outer conductor contact (part numbers PE 9002 and PE 9127). The level of system residual IM when testing these connectors gave a maximum measurement error of 2 dB.
- Pasternack Enterprises "standard" $N$-type connectors with gold-plated inner conductor contact and outer conductor contact of nickel (PE 9311) or stainless steel (PE 9426). The level of system residual IM when testing these connectors gave a maximum measurement error of 0.2 dB.

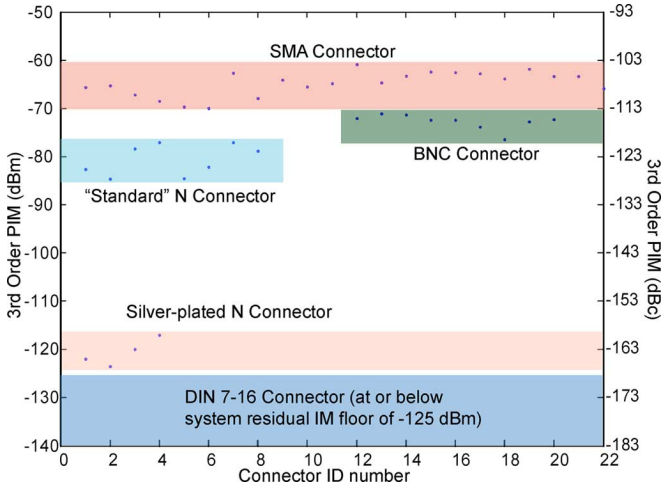


Fig. 5. Ranges of third-order IM power output by different types of coaxial connections in a two-tone test with $2 \times 43$ dBm forward power at carrier frequencies of 463 and 468 MHz. Shaded bands denote the range of the IM generated by a connector family. Dots inside these bands are the IM produced by individual connections.

- Spinner GmbH $N$ type with silver-plated inner and outer conductor contacts (part numbers BN 950890 and BN 203834). The level of system residual IM when testing these connectors gave a maximum measurement error of $-8$ or $+4$ dB.
- Spinner GmbH DIN 7–16 connectors with silver-plated inner and outer conductor contacts (BN 756404 and BN 203391). The IM of these connectors is less than the residual IM of our measurement system, therefore, Fig. 5 shows the upper bound on the IM these connectors could generate.

The results of this study are summarized in Fig. 5. Here each dot on the graph represents the IM produced by an individual connection. The range defined by the IM of these connections is shown by the darkened bands. It is notable that the IM levels of the different families of connectors are distinct, with the average IM level of different connector families varying by tens of decibels. Therefore, an individual connection's expected IM level can be estimated roughly by the ranges in Fig. 5 without having to test it individually.

Although hardly rigorously proven here, we also note the general trend that as a connector increases in size, the IM level of the connection decreases. This is most clear when comparing the SMA to standard $N$-type connectors, which have similar metallic composition, but very distinct IM levels. We also see a great difference in IM levels between the "standard" and silver-plated $N$ connections, which shows a dependence of IM level on metal composition, as has been noted for other structures in [9]. These two families of connectors are essentially identical in geometry, yet the IM of the silver-plated $N$ connectors is at least 30 dB less than that of the "standard" type, which has a gold-plated center pin and nickel or stainless-steel outer contact.

### B. Stability of PIM Output

For the analysis given in Section II, we assume the IM output of a coaxial connection to be constant with time. However, PIM

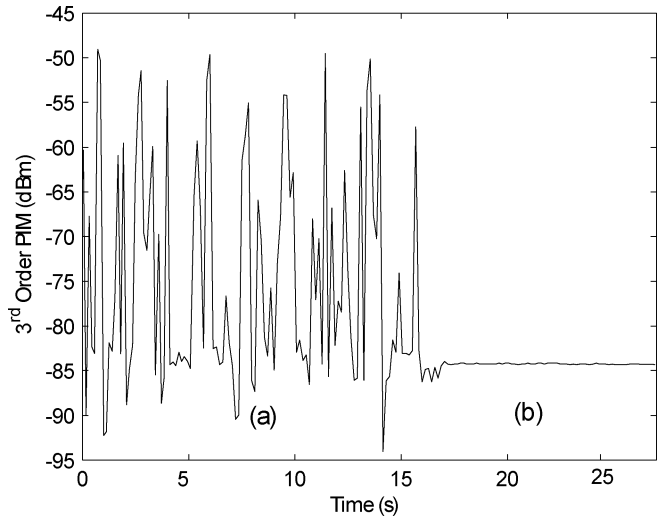


Fig. 6. Time plot of the PIM produced by: (a) a loosely connected and (b) a fully tightened "standard" $N$ connector.

in RF components including connectors has shown a high sensitivity to environmental factors such as transient stresses [10]. Such transient IM behavior cannot be predicted as yet since the underlying causes of PIM in coaxial connectors are not known. Therefore, in order to successfully predict the IM level in high-power systems, the transient component of the IM output of a coaxial connection must be considered negligible (i.e., the IM of a connection must be assumed constant with time) as long as the power and frequency of the signal passing through the connectors is constant. This section seeks to establish the conditions under which this approximation is valid.

Fig. 6 shows the IM of a "standard" $N$ connector as a function of time. For the first 16 s, the connector is loosely connected and tightened down in (a), and is fully tightened thereafter in (b). When the connector is loosely connected in (a), the IM of this connector had a broadly variable (40 dB) transient behavior. In contrast, when properly tightened to the correct torque and immobilized, the IM of the connector was constant with time. Therefore, care must be taken so that the torsion stress exerted on the coaxial connection is small, especially in the case of small connector types like SMA. However, it is reasonably simple to assure this condition in our experimental setup, and thus, for the experiments in this paper, we take the IM of a coaxial connection to be constant with respect to time.

Another source of time variance in the IM produced by a coaxial connector is the fact that the IM level of a connector changes from connection to connection. While we have found this to be true, this change in the IM level is quite small, even when more connections than the specified number for a connector's lifetime are made. We measured the IM level of an SMA connector as it was cycled through 50 disconnect/reconnect cycles (as SMA connectors are only rated for a "very limited number of connection cycles" [11], 50 cycles was thought sufficient to probe the connector's IM behavior over a normal lifetime). The distribution of IM power varied over a narrow range with a standard deviation of just 0.24 dB without a trend toward either increasing or decreasing. Therefore, we also treat the IM produced by a coaxial connector to be constant from connection to connection.

## IV. IM Dependence on Power Delivered Through the Connection

One of the most interesting aspects of PIM is the anomalous less than 3-dB/dB regrowth rate of the third-order IM product with respect to input power $P_{\rm in}$ (in this study, $P_{\rm in}$ will refer to the power in either one of the equal-power carrier tones). Although not yet fully understood from a physical perspective, many investigators have noted this behavior as reported in [2], [12], and [13]. Here, we present two methods of accounting for the power dependence of the PIM produced by coaxial connectors. The first method involves fitting a multiorder polynomial current versus voltage (*I–V*) curve to the measured IM power ($P_{\rm IP}$) versus $P_{\rm in}$ curve of a coaxial connector. The second method is an *I–V* curve based on the hyperbolic tangent function. This method is able to predict the IM level of coaxial connectors over broad ranges of input power with far fewer fitting parameters (coefficients of the terms of the nonlinear function) than required for the first method.

### A. Polynomial-Series-Based I–V Curves

Due to its ease of use, the first attempt of describing a nonlinear system usually takes the form of a polynomial series. Below we will describe how a polynomial series expansion can be made to model the $P_{\rm IP}$ versus $P_{\rm in}$ curve of a coaxial connection or other PIM-producing component.

A first model of a nonlinear device's *I–V* curve is typically a simple polynomial series

$$I(V) = b_1 V + b_3 V^3 + b_5 V^5 + b_7 V^7 \cdots. \tag{9}$$

Given an input signal where both input tones have the same magnitude,

$$V(t) = A\left[\cos(\omega_1 t) + \cos(\omega_2 t)\right] \tag{10}$$

the harmonic and IM frequencies can be obtained through direct expansion of (9) [14]. Although the total expansion gives all harmonics and IM products generated by a nonlinearity described by (9), for simplicity, in the following analysis, we will focus on the lower sideband third-order IM at frequency $2f_1 - f_2$. An expression for the voltage of this IM is found by substituting (10) into (9), expanding, and collecting all the terms containing a factor $\cos[(2\omega_1 - \omega_2)t]$. The average power at this frequency is then found to be

$$P_{\rm IP} = \left[A^3 a_3 + A^5 a_5 + A^7 a_7 \cdots\right]^2 \tag{11}$$

where $a_n$ is proportional to $b_n$ for $n = 3, 5, 7, \ldots$.

The IM power versus input power ($P_{\rm IP}$ versus $P_{\rm in}$) curves of common electronic nonlinear components such as amplifiers usually obey the relation

$$P_{\rm IP} \propto A^{2n} \tag{12}$$

where $n$ is the order of the IM, and $A$ is the magnitude of the voltage of the input tones, as used in (10) and (11). However, this simple behavior has been found not to hold for many PIM-producing components, including coaxial connections. For these

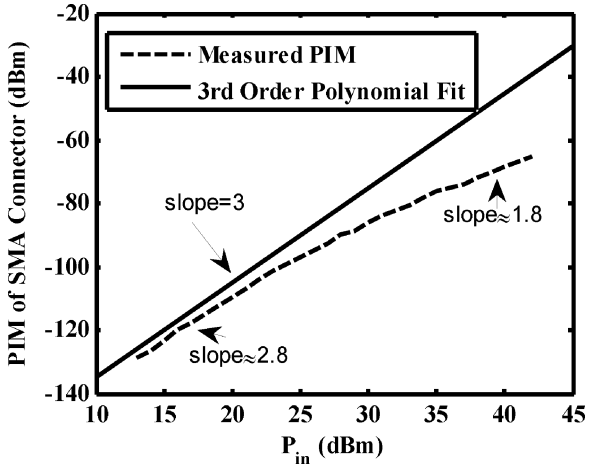


Fig. 7. $P_{\rm IM}$ versus $P_{\rm in}$ curve for an SMA connection measured on a Summitek SI-400C PIM analyzer (dotted line). Also shown is a fit to this curve based on a third-order Taylor expansion of the *I–V* curve.

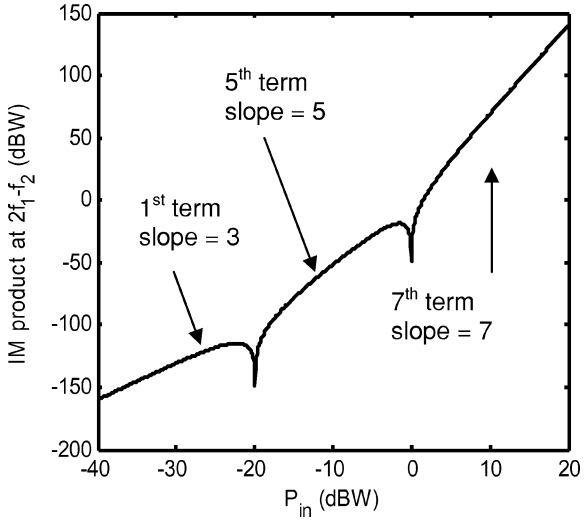


Fig. 8. Nulls occur in (11) due to interference between the three terms.

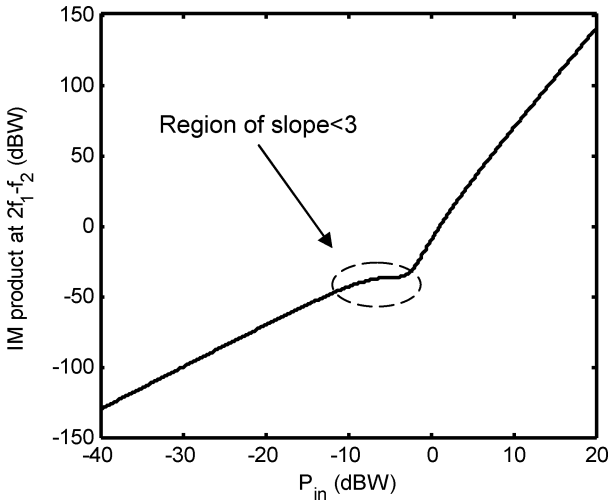


Fig. 9. Nulls in Fig. 8 come together and interfere, causing a broad region of less-than predicted slope.

devices, the regrowth rate, $n$ in (12), is usually less than the order of the IM, and in fact, is not constant with respect to input power [2], [13]. This behavior in an SMA coaxial connection is shown in Fig. 7, which plots the measured IM of an SMA connection under a two-tone test as the power in both carriers was swept from 13 to 43 dBm.

A single-term third-order polynomial that loosely fits this behavior is also shown as a straight line in Fig. 7. As can be seen, the simple third-order polynomial obeys the characteristic of (12). Since the IM level of the SMA connection does not obey (12), a single-term third-order *I–V* curve is not a good model of the power dependence of the IM generated by this connection. To achieve the measured behavior shown in Fig. 7, polynomial-based *I–V* curves for coaxial connections necessarily contain many terms. As a first step toward constructing a polynomial *I–V* curve to fit the measured $P_{\rm IP}$ versus $P_{\rm in}$ curve shown in Fig. 7, let us examine Fig. 8, where (11) is plotted as a function of power input.

In constructing this graph, we chose $a_3$, $a_5$, and $a_7$ such that the ratio $a_3/a_5$ was $-0.01$ and $a_5/a_7$ was $-1$, resulting in the nulls at $-20$ and 0 dBW. These nulls are a result of the interference between orders of the polynomial (11) (there is a sequential sign change from $a_3$ to $a_5$ to $a_7$). Nulls such as these have been observed in active nonlinear devices, such as in [15]. We see three distinct regions separated by nulls in the IM power in Fig. 9. Near the nulls, the simple regrowth law (12) is not upheld, but only over a small range (approximately 3 dB) of input power. Contrarily, the behavior of the SMA connection shown in Fig. 7 contradicts the prediction of (12) over a large range of input powers. There are also no nulls observed in the SMA data shown in Fig. 7. To achieve the necessary reduction of slope from that predicted by (12) while avoiding the nulls seen in Fig. 8, we allow three or more terms of the polynomial *I–V* expansion (11) to interfere simultaneously. The coefficients $a_3, a_5$, and $a_7$ are adjusted so that the two nulls observed in Fig. 4 move together and merge. The result of this three-term interference can be seen in Fig. 9—the two nulls disappear, and we are left with a short region over which slope is less than 3, similar to that of the measured $P_{\rm IP}$ versus $P_{\rm in}$ curve shown in Fig. 7, but for a much narrower range (approximately 10 dB) of input power.

The third–fifth–seventh-order interference shown in Fig. 9 begins to approximate the behavior of the real IM measurement shown in Fig. 7. Thus, by adding more terms of progressively higher order to (1), a polynomial series can be used to model the $P_{\rm IP}$ versus $P_{\rm in}$ behavior of coaxial connections. As an example, a 24-term 49th-order polynomial *I–V* curve fit to the $P_{\rm IP}$ versus $P_{\rm in}$ characteristic of an SMA connector is shown in Fig. 10.

Two drawbacks to using this approach are apparent. In the first case, we required the interference of three odd-order polynomial terms to produce the local departure from (12)-type behavior seen in Fig. 9. The number of orders required to span the 30-dB input power range covered in Fig. 8 is rather large. The second drawback is a well-known problem with polynomial fitting expressions: beyond the range of $P_{\rm in}$ where the fitting function is valid, it begins to diverge rapidly, as can be seen in the upper right corner of Fig. 10. However, within the range

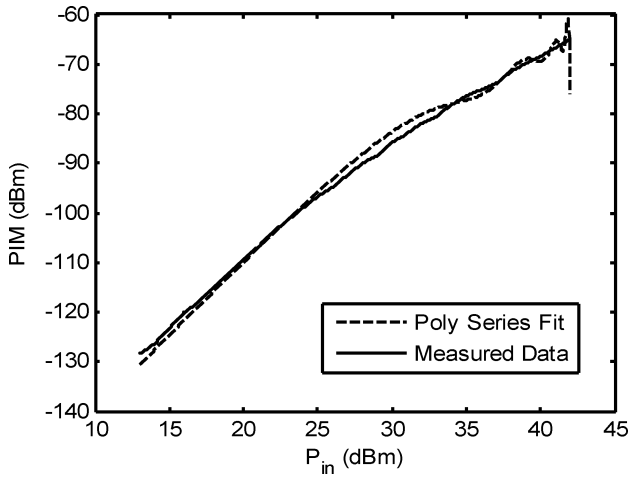


Fig. 10. Measured $P_{\rm IP}$ versus $P_{\rm in}$ curve of an SMA connector under two-tone test, along with a fit provided by a 24-term 49th-order polynomial *I–V* curve.

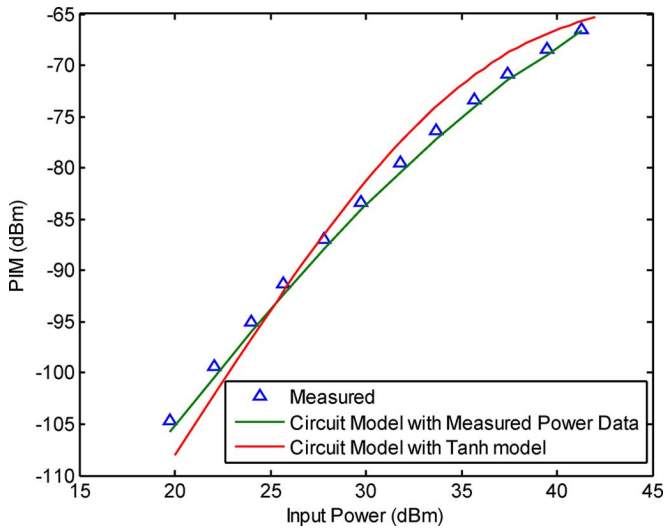


Fig. 11. Measured $P_{\rm IP}$ versus $P_{\rm in}$ (triangles) of the network shown in Fig. 11 along with the IM predicted utilizing the circuit model and $P_{\rm IP}$ versus $P_{\rm in}$ data of individual connections (dotted line) and the circuit model where the $P_{\rm IP}$ versus $P_{\rm in}$ dependence is predicted by the hyperbolic-tangent-based *I–V* curve (13) (solid line).

of power measured, we find that the 24-term polynomial series agrees well with the measurement

### B. Hyperbolic Tangent-Based I–V Curves

The hyperbolic tangent function has been used as a prototypical nonlinear device model by Carvalho and Borges [14]. More recently, Macchiarella and Sartorio [16] employed the hyperbolic tangent as a model for describing behavior of IM produced by coaxial resonators. Specifically, an *I–V* curve given by

$$I = g_0 \left[V + k_1 \tanh(k_2 V)\right] \tag{13}$$

was used by Macchiarella and Sartorio to describe the curve of $P_{\rm IP}$ versus $P_{\rm in}$ in coaxial resonators, where $g_0$ is adjusted to give the correct linear impedance of the device, and $V$ is the input voltage. A reasonable fit to the $P_{\rm IP}$ versus $P_{\rm in}$ characteristic of an SMA connection can be made by adjusting the parameters $k_1$ and $k_2$.

We have found the model (13) to adequately describe IM behavior of coaxial connections over large ranges of input power $P_{\rm in}$. Fig. 11 in Section V shows the prediction given when using this expression to model the *I–V* curves of the point nonlinearities in a test network. In contrast to the polynomial series, which requires tens of independent parameters to model this curve, the model based on (13) is able to follow the data curve closely over a 30-dB input power domain and a range of 70 dB by optimizing only two independent parameters $k_1$ and $k_2$.

## V. Experimental Verification

The main purpose of this paper has been to demonstrate that once the IM level of all individual components have been characterized, the total IM output of a network can be calculated by circuit theory, treating the coaxial connectors as point nonlinearities separated by transmission lines. By measuring the IM produced by an RF network's components and the electrical distances separating nonlinearities, we can use (1) and (2) to construct expressions like (8), which accurately predict the total IM output of a system. The excellent agreement of the cascade of

Fig. 12. Network used to verify the technique of predicting the IM distortion product of a system due to coaxial connectors.

coaxial connectors shown in Fig. 4 can be taken as a verification of both the techniques described and the assumptions taken herein. However, as a more comprehensive example that includes one of the models of the power-dependence of IM power described in Section IV, a mixed network of connectors, cables, soldered connections, and a microstrip line was assembled and is pictured in Fig. 12. The coaxial connections in this network were: four DIN 7–16, four $N$-type connections, one BNC, and one SMA. The IM level of the individual connectors was measured at a range of input power from 13 to 42 dBm per input tone in a two-tone test. The electrical lengths separating the nonlinear coaxial connections were calculated by measuring each component's physical length and by dividing this by the wavelength in the component. A circuit model was constructed using the technique outlined in Section II.

We compare the cases where the power dependence is accounted for using: (a) measured data of the $P_{\rm IP}$ versus $P_{\rm in}$ characteristic of each connection measured by itself and (b) the two-parameter $P_{\rm IP}$ versus $P_{\rm in}$ curve fit based on (13). The predictions of each of these models are compared against the measured values of the IM of the test network in Fig. 11. The total PIM output of the system is dominated at low input power by the single SMA connector in the assembly. Then as power is increased, the increasing PIM output of the BNC connector begins to destructively interfere with that of the SMA connector, resulting in a lower total PIM (2.7 dB) output than would result

from the SMA connector alone. This 88% drop in IM power due to the interference of the multiple sources of PIM is predicted accurately by the model.

For the circuit model whose $P_{\mathrm{IP}}$ versus $P_{\mathrm{in}}$ values are taken directly from measurement of the individual connections, we see good agreement over the 22-dB range of power measured (maximum error of 1.1 dB) and reasonable agreement between predicted and measured values when the power dependence of the IM produced by each connection is accounted for by (13) with a maximum error of 2.7 dB. This accuracy indicates that the point nonlinearities of the coaxial connectors dominate the PIM response of the DUT over the entire range of powers we measured, and that the behavior of the IM distortion of the network as a whole is reasonably captured by our model.

## REFERENCES


[1] V. Golikov, S. Hienonen, and P. Vainikainen, "Passive intermodulation distortion measurements in mobile communication antennas," in *Veh. Technol. Conf.*, 2001, vol. 4, pp. 2623–2625.

[2] P. L. Lui, "Passive intermodulation interference in communication systems," *Electron. Commun. Eng. J.*, vol. 2, pp. 109–118, Jun. 1990.

[3] R. Timsit, "High speed electronic connectors: A review of electrical contact properties," *IEICE Trans. Electron.*, vol. E88-C, pp. 1532–1545, Aug. 2005.

[4] R. Hartman, "Passive intermodulation analyzers-D configuration," Summitek Instrum., Engelwood, CO, Tech. Data, 2007. [Online]. Available: http://www.summitekinstruments.com/passive/docs/Technical%20Data%20D.pdf

[5] B. Deats and R. Hartman, "Measuring the passive-IM performance of RF cable assemblies," *Microw. RF Eng.*, vol. 36, pp. 108–114, 1997.

[6] Y. Yamamoto and N. Kuga, "PIM characteristics of resistive dummy loads," in *Proc. Asia–Pacific Microw. Conf.*, Dec. 2005, vol. 5.

[7] S. Hienonen and A. V. Raisanen, "Effect of load impedance on passive intermodulation measurements," *Electron. Lett.*, vol. 40, pp. 245–247, Feb. 2004.

[8] J. A. Jargon *et al.*, "NIST passive intermodulation measurement comparison for wireless base station equipment," in *52nd ARFTG Conf. Dig.*, 1998, pp. 128–139.

[9] F. Arazm and F. A. Benson, "Nonlinearities in metal contacts at microwave frequencies," *IEEE Trans. Electromagn. Compat.*, vol. 22, no. 8, pp. 142–140, Aug. 1980.

[10] R. Hartman, "Passive intermodulation measurement techniques," Summitek Instrum., Englewood, CO, 1999. [Online]. Available: http://www.summitekinstruments.com/passive/docs/pimprimer.pdf

[11] "Connector care," Agilent Technol., Palo Alto, CA, 2007. [Online]. Available: http://na.tm.agilent.com/pna/connectorcare/connector_care.pdf

[12] C. V. Quiles, B. Mottet, and H. L. Hartnagel, "PIM analysis at waveguide flanges: A theoretical approach," in *Proc. 4th Int. Multipactor, Corona, Passive Intermodulation in Space RF Hardware Workshop*, Sep. 2003. [Online]. Available: http://conferences.esa.int/03C26/papers/a024.pdf

[13] E. M. Rutz-Phillip, "Power conversion in nonlinear resistive elements related to interference phenomena," *IBM J.*, vol. 11, pp. 544–552, Sep. 1967.

[14] N. B. Carvalho and J. C. Pedro, *Intermodulation Distortion in Microwave and Wireless Circuits*. Norwood, MA: Artech House, 2003, pp. 11–22.

[15] M. J. Bailey, "Intermodulation distortion in pseudomorphic HEMTs and an extension of the classical theory," *IEEE Trans. Microw. Theory Tech.*, vol. 48, pp. 104–110, Jan. 2000.

[16] G. Macchiarella and A. Sartorio, "Passive intermodulation in microwave filters: Experimental investigation," in *IEEE MTT-S Int. Microw. Symp. Dig. WMB-7 Filter II Workshop*, Long Beach, CA, Jun. 2005. [Online]. Available: http://maxwell.uwaterloo.ca/~myu/publications/WMB-7-color-Macchiarella.pdf


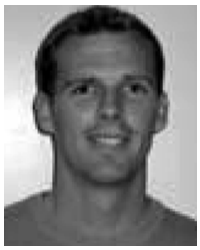

**Justin Henrie** (S'07) was born in Salt Lake City, UT. HE received the B.S. degree in electrical and computer engineering from Brigham Young University, Provo, UT, in 2005, and is currently working toward the Ph.D. degree at Purdue University, West Lafayette, IN.

He is currently a Graduate Research Assistant with the IDEAS Laboratory, Electrical and Computer Engineering Department, Purdue University.

**Andrew Christianson** (S'05) was born in Denver, CO. He received the B.S. degree in electrical and computer engineering from Purdue University, West Lafayette, IN, in 2005, and is currently working toward the Ph.D. degree at Purdue University.

He is currently a Graduate Research Assistant with the IDEAS Laboratory, Electrical and Computer Engineering Department, Purdue University.

**William J. Chappell** (S'98–M'02) received the B.S.E.E., M.S.E.E., and Ph.D. degrees from The University of Michigan at Ann Arbor, in 1998, 2000, and 2002, respectively.

He is currently an Assistant Professor with the Electrical and Computer Engineering Department, Purdue University, West Lafayette, IN, and is also a member of the Birck Nanotechnology Center and the Center for Wireless Systems and Applications. His research focus is on advanced applications of RF and microwave components. He has been involved with numerous Defense Advanced Research Projects Agency (DARPA) projects involved in advanced packaging and materials processing for microwave applications. His research sponsors include Homeland Security Advanced Research Projects Agency (HSARPA), Office of Naval Research (ONR), National Science Foundation (NSF), the State of Indiana, Communications-Electronics Research, Development, and Engineering Center (CERDEC), U.S. Army Research Office (ARO), as well as industry sponsors. His research group uses electromagnetic analysis, unique processing of materials, and advanced design to create novel microwave components. His specific research interests are the application of very high-quality and tunable components utilizing package-scale multilayer components. In addition, he is involved with high-power RF systems, packages, and applications.

Dr. Chappell was the recipient of the URSI Young Scientist Award, the Joel Spira Teaching Excellence Award, and the Eta Kappa Nu 2006 Teacher of the Year Award presented by Purdue University.